The Reynolds Number Influence on the Flow Over Shallow Cavities

Paulo S.B. Zdanski
Instituto Tecnológico de Aeronáutica, CTA/ITA/IEAA, S. J. Campos, SP, 12228-900,
zdanski@aer.ita.br

M. A. Ortega
Instituto Tecnológico de Aeronáutica ,CTA/ITA/IEAA, S. J. Campos, SP, 12228-900,
ortega@aer.ita.br

Nide G. C. R. Fico Jr.
Instituto Tecnológico de Aeronáutica ,CTA/ITA/IEAA, S.J. Campos, SP, 12228-900,
nide@aer.ita.br

Abstract. This work investigates the Reynolds number influence upon the flow inside a two dimensional shallow cavity. The flow regime varies from laminar to turbulent. The numerical method used is based upon the SIMPLER algorithm. Turbulence closure is accomplished with the aid of the standard k-å model. It was observed that increasing the Reynolds number affects the flow topology in distinct ways depending upon the flow regime, laminar or turbulent.

key words: Incompressible flow, shallow cavity, solar energy, numerical methods.

1. INTRODUCTION

The flow over cavities is of great interest as it is related to various engineering applications: cooling of electronic devices, combustion chambers and heat loss that occur on the upper surface of a solar energy collector are a few examples. Most of the work found in the literature deals with cavities of small aspect ratio. Aung (1983) found, experimentally, that for laminar forced convection, the local heat transfer distribution on the cavity floor has a maximum value located between the midpoint of the cavity floor and the downstream wall. Bath and Aung (1984) numerically simulated the two-dimensional, laminar flow over cavities and showed that the heat transfer inside the cavity is a function of its aspect ratio. Sinha et al. (1982) made an experimental study of the flow over cavities of various aspect ratios. In their work these authors classified the cavity as open or closed based upon the number of re-circulating bubbles formed and the position that they occupy inside the cavity. Pereira and Sousa (1995) studied both numerically and experimentally the unsteady flow inside cavities. Thus, little effort has been putted into high aspect ratio cavities, which are the main focus of the present work. Such cavities have an interesting application for studying the flow over flat plate solar energy collectors with wind barrier (Zdanski et al., 2000). The present effort is, therefore, related to numerical analysis of two-dimensional flow over shallow cavities. The Reynolds number influence upon the flow topology was considered for both, laminar and turbulent cases.

2. MATHEMATICAL MODEL AND NUMERICAL METHOD

The mathematical model considered here is the two-dimensional, incompressible, Navier-Stokes equations written for a Cartesian coordinate frame. To account for the turbulent transport of

momentum, without penalizing excessively the CPU time and the computer memory, the Reynolds-Averaged Navier-Stokes equations were used.

The Boussinesq hypothesis was invoked to relate the Reynolds stress tensor to the mean flow velocity gradient. In the context of the standard k-ε turbulence model, the eddy viscosity is given by the expression

$$m_T = C_m r \frac{k^2}{e} \,, \tag{1}$$

where C_m is an empirical constant and 'k' is the turbulent kinetic energy which is given by

$$\frac{\partial(rk)}{\partial t} + \frac{\partial(ru_i k)}{\partial x_i} = \frac{\partial}{\partial x_i}\left[\left(\frac{m_T}{s_k}\right)\frac{\partial k}{\partial x_i}\right] + rG - re \,. \tag{2}$$

Similarly, the rate of change of the turbulent energy dissipation, 'ε', is modeled by

$$\frac{\partial(re)}{\partial t} + \frac{\partial(ru_i e)}{\partial x_i} = \frac{\partial}{\partial x_i}\left[\left(\frac{m_T}{s_e}\right)\frac{\partial k}{\partial x_i}\right] + C_1 r \frac{e}{k} G - C_2 r \frac{e^2}{k} \,, \tag{3}$$

being G the term that represents the generation rate of turbulent kinetic energy, that is,

$$G = \frac{m_T}{r}\left[\left(\frac{\partial u_i}{\partial x_j} + \frac{\partial u_j}{\partial x_i}\right)\frac{\partial u_i}{\partial x_j}\right] \,. \tag{4}$$
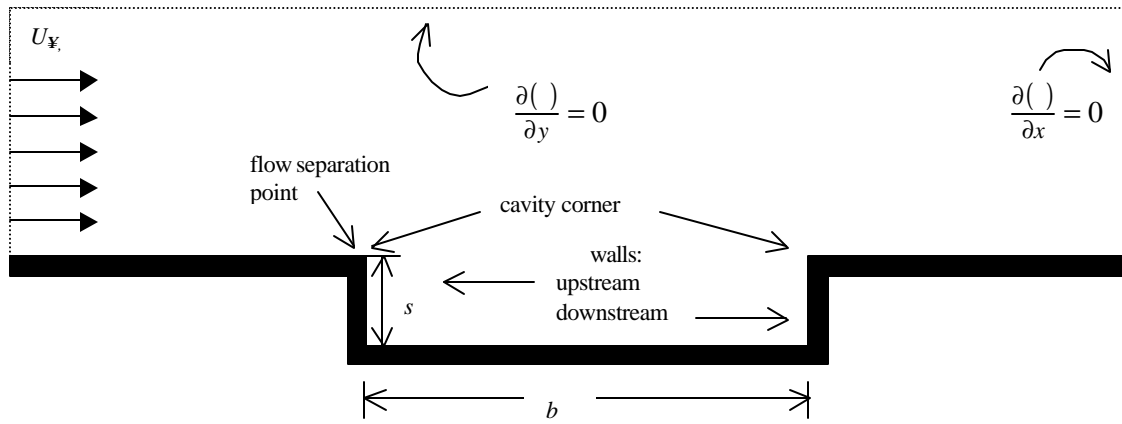
The five empirical constants that appear at eqs. (1), (2) and (3) are those suggested by Launder and Spalding (1972)

$$s_k = 1.0 \,; \; s_e = 1.3 \,; \; C_m = 0.09 \,; \; C_1 = 1.44 \,; \; C_2 = 1.92 \,. \tag{5}$$

The partial differential equations were written in a discrete form using the finite volume technique and the resultant system of algebraic equations are solved by the SIMPLER algorithm (Patankar, 1980) on a staggered grid.

2.1 Boundary conditions

Figure (1) shows, schematically, the problem geometry, its nomenclature as well as some indication of the boundary conditions enforcement. The cavity depth is denoted by s, while its length is indicated by b. At the entrance plane, all the variables are fixed except the pressure that is extrapolated from inside. The oncoming velocity profile is uniform, as seen on Fig. (1). Other flow variables, such as the turbulence intensity level, and the turbulent dissipation are also kept fixed at the computational domain inlet plane. At the exit section, as well as at the upper boundary, a parabolic boundary condition is used. This is equivalent on saying that the property derivatives are all zero at these boundaries. A parabolic boundary condition is interesting in the sense that it is non-reflexive. Finally, at the solid walls the no-slip boundary condition is enforced, that is, u and v equal to zero. At the solid walls, special treatment is required in terms of the turbulence model used. The gap between the first computational grid point and the wall is bridge using wall laws. In this sense the first computational grid point, in the direction normal to the walls, must be placed outside the laminar sub-layer of the turbulent boundary layer.

$$\frac{\partial(\ )}{\partial y}=0$$

$$\frac{\partial(\ )}{\partial x}=0$$

U_∞

flow separation point

cavity corner

walls:
upstream
downstream

s

b

Figure 1: Problem geometry, nomenclature and boundary conditions.

2.2 Computational grid

A typical computational mesh is shown in Fig. (2). The computational domain is sub-divided in two by an orthogonal, non-uniform mesh. The grid was refined close to the walls and to the cavity entrance and exit planes where the greatest property gradients are expected. Grid stretching was always smaller than 10 % to avoid numerical errors. The points above the cavity form the upper mesh while points inside the cavity pertain to the lower mesh. Special treatment is given to the two volumes located at the cavity corners (Zdanski, 2001). The inlet boundary is located at three cavity depths (3s) upstream of the separation point. The outlet boundary is placed at a distance of 4s from the downstream wall. Due to the parabolic character of the upper boundary, numerical experiments showed that, a minimum of 5s was necessary in order to avoid spurious interference on the numerical solution.
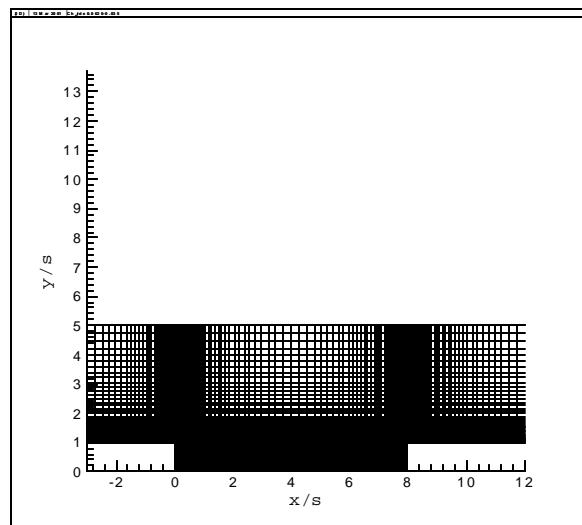

Figure 2: Typical computational grid.

3. RESULTS

The primary objective of the present work is to analyze the influence of the Reynolds number, based upon the cavity depth, Re_s, on the flow topology inside 2-D cavities of high aspect ratio. The study covers both laminar and turbulent flow regimes. The numerical code used for such analysis was developed by CFD group at the Aerodynamics Department of the Instituto Tecnológico de

Aeronáutica and it has been carefully validated in previous work (Zdanski et al, 2000 and Zdanski, 2001).

3.1 Laminar flow.

The cavity used for the laminar flow simulations had an aspect ratio. *b/s*, equal to twelve. The Reynolds number, based on a cavity depth of *0.625* cm, varied from *147* to *662*. In this range it was found that two re-circulating bubbles were always formed inside the cavity. Nevertheless, their position along the cavity as well as their shape varied with Re_s.
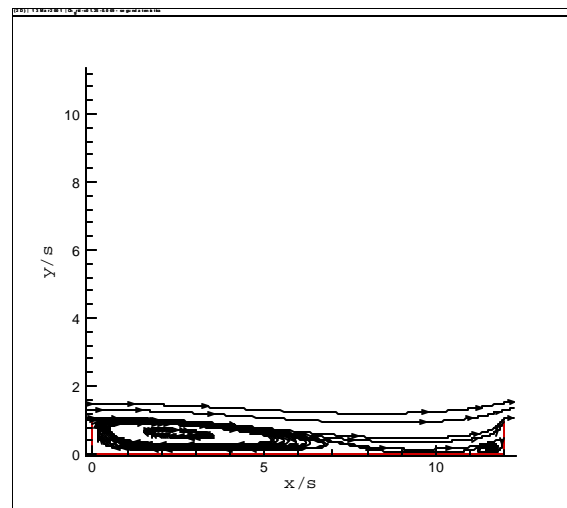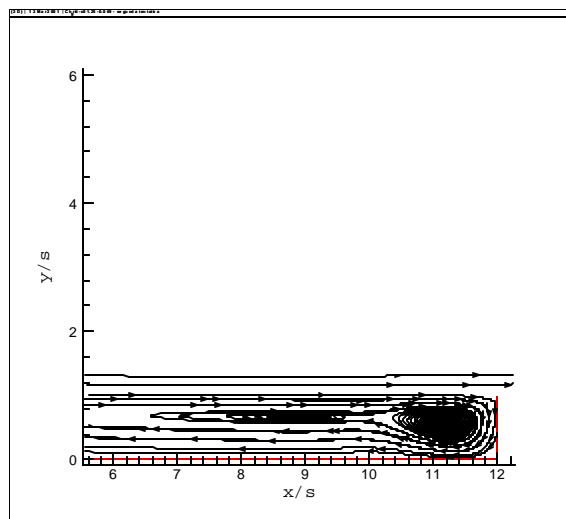

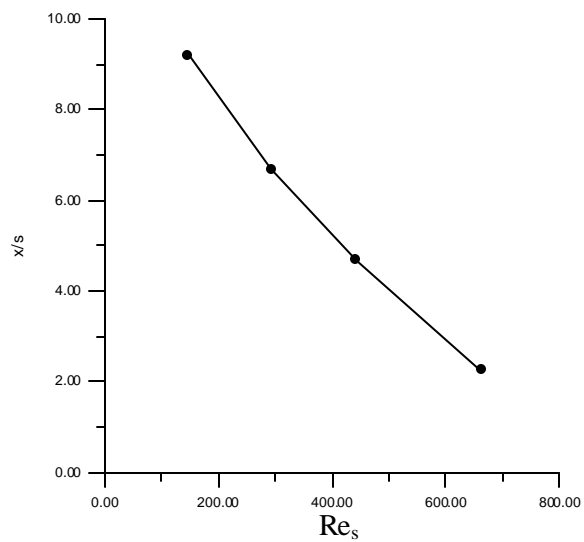**Figure 3:** Streamlines for the case of Reynolds number equal to 147.
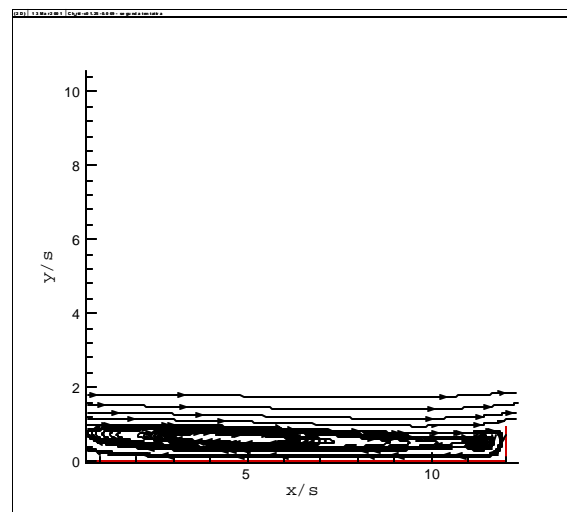
Figure 4: Streamlines for the case of Reynolds number equal to 294.
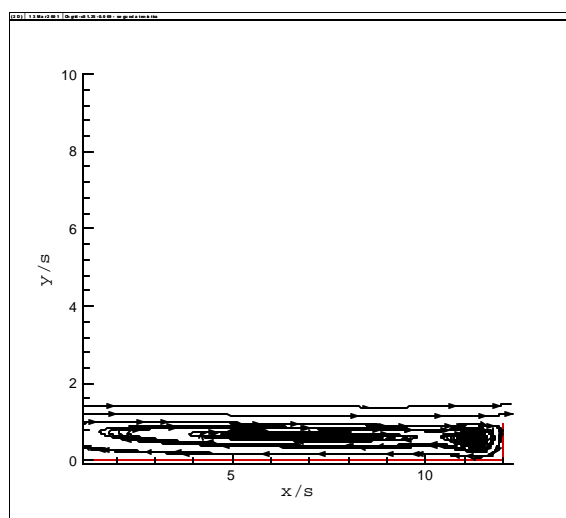
Figure 5: Streamlines for the case of Reynolds number equal to 442.

Figure 6: Streamlines for the case of Reynolds number equal to 662.


**Figure 7:** Distance from the centers of the two bubbles as a function of Reynolds number, Re_s.

The lower Reynolds number considered is equal to 147 and corresponds to a free stream velocity of *0.4 m/s*. As see in Fig. (3), the oncoming flow penetrates the cavity touching its bottom around *x/s=8.5*. The two bubbles are well defined and the flow is reversed along parts of the cavity floor. The bubble closer to the upstream wall has its center at $x/s \approx 2.4$, while the one near the downstream wall is centered at $x/s \approx 11.6$. As the Reynolds number was increased the centers of the two bubbles moved closer to each other, as figs. (3) to (6) show clearly. For the highest Reynolds number investigated, $Re_s= 662$, the center of the bigger re-circulating bubble was found to be at $x/s \approx 8.9$. On the other hand, the smaller one barely moved its center appearing at $x/s \approx 11.1$. It is also interesting to notice, examining figs. (3) to (6), that the aspect of the bigger bubble increases with the Reynolds number. As for the smaller bubble, closer to the downstream wall, it is apparent that its size increases with Re_s. Both, the approximation of the centers as well as the change in the bubble shape, may be associated with the inertia of the oncoming flow, that is, its ability to penetrate into the cavity. Figure (7) presents the plot of the distance between the centers of the two bubbles, for laminar flow, against Re_s. It is clear that the bubbles are closer as the oncoming flow velocity and, consequently, the Reynolds number is increased.

3.2 Turbulent Flow

Most flows of interest are turbulent. To the author's knowledge very little work has been done on high aspect ratio shallow cavities. Therefore, besides the flow streamlines other results involving important flow variables such as turbulent kinetic energy and pressure are reported hereafter. The particular cavity investigated had an aspect ratio equal to eight. The turbulence level of the oncoming flow was equal to 4% of the kinetic energy of the undisturbed mean flow for all Reynolds numbers considered in this effort. Three values for inlet free stream velocity were used: 5, 8, and 12 m/s. These values correspond to $Re_s= 11765$, 18823, and 28235, respectively.
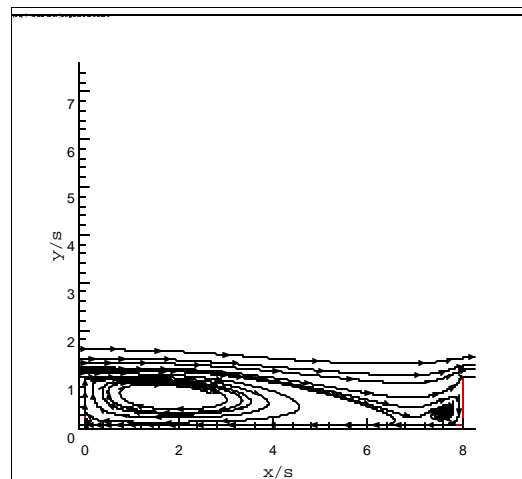
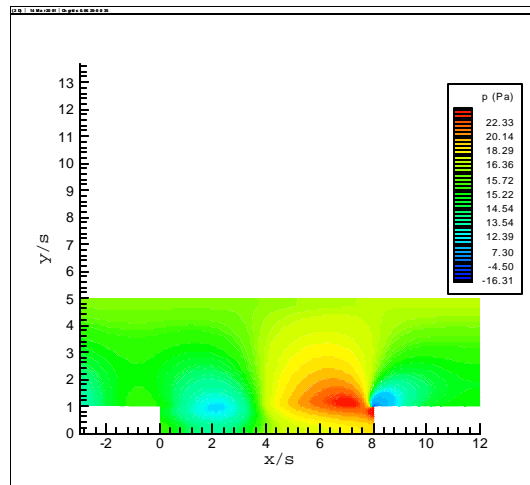**Figure 8:** Streamlines for the case of Reynolds number equal to 11765.
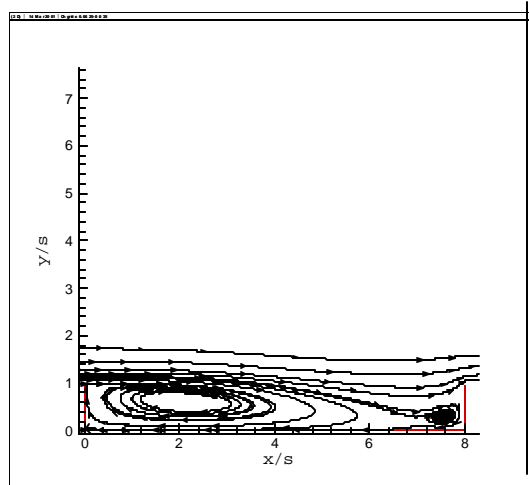
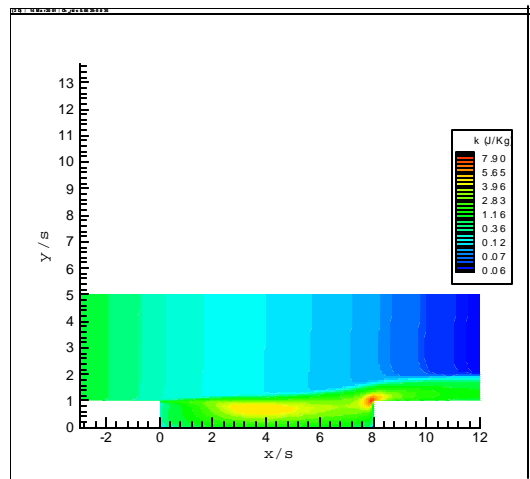**Figure 9:** Streamlines for the case of Reynolds number equal to 18823.
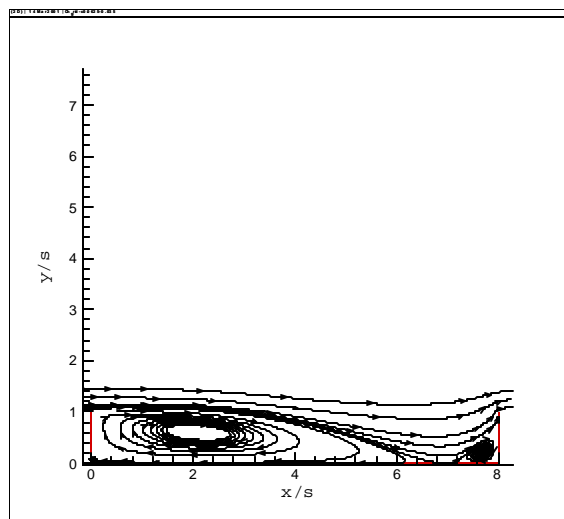
Figure 10: Streamlines for the case of Reynolds number equal to 28235.

For most of the numerical experiments undertaken, the number of volumes of the two meshes, one for the domain above the cavity and the other for the cavity itself, typically added up to 9000. The first point off the wall was located around $y^+ = \frac{yu}{n} \approx 30$, that is, compatible with a high Reynolds number turbulence model. Figures (8) to (10) show the streamlines for the three Re_s studied. Comparing these figures it is apparent that, for turbulent flows, the Reynolds number does not influence the position of the bubbles' center considerably, unlike laminar flows. It is interesting to point out that only for the higher value of the Reynolds number investigated, $Re_s = 28235$, a reattachment point inside the cavity appears. This fact is related to the greater vorticity level associated with the highest Re_s, at the separation point. More specifically, the higher the vorticity the more "energetic" the first re-circulation bubble becomes and, therefore, more capable of deflecting the oncoming flow towards the cavity floor.

Figure 11: Pressure contours for the case of Reynolds number equal to 18823.

Figure (11) shows the pressure distribution along the whole computational domain for $Re_s=$ 18823. As it can be observed, the pressure variation is around 40 Pascal. Nevertheless, it is clear that there is a well-defined higher-pressure region that corresponds to the flow stagnation at the downstream wall. Further, the lowest pressures in the flow filed are associated with the center of the greater re-circulation bubble ($x/s \approx 2$) and also with the re-circulation zone due to flow separation at $x/s = 8$.

Figure 12: Kinetic energy contours for the case of Reynolds number equal to 18823.

Figure (12) displays the turbulent kinetic energy, k, also for $Re_s=$ 18823. At the separation point a shear layer is originated, contributing to a high values of the turbulent kinetic energy. Inside the cavity the region the diffusive nature of the fluid is responsible for the large region of high values of k. Once again, the downstream wall is associated with the peak of a property, the turbulent kinetic energy in this case, because of the high gradients appearing in the region.

4. CONCLUSION

The numerical simulation of flows, both laminar and turbulent, over 2-D shallow cavities with high aspect ratio was successfully performed. The results showed that the flow topology inside such cavities is influenced by the variation of the Reynolds number. However, laminar and turbulent flows seem to be affected in different ways. For the former both the shape of the re-circulating

bubbles as well as the distance between their centers were found to be a function of Res. For the latter, however, the most important difference upon the flow caused by the increase of the Reynolds number was the appearance of a reattachment point at the cavity floor. Particularly for turbulent flows, it was found that the corner of the downstream wall presented peaks for both the pressure and the turbulent kinetic energy.

5. ACKNOWLEDGEMENTS

6. REFERENCES

Aung, W. and Bhatti, A., 1984, "Finite Difference Analysis of Laminar Separated Forced Convection in Cavities", Journal of Heat Transfer, Vol.106, pp. 49-54.

Aung, W., 1984, "An Interferometric Investigation of Separated Forced Convection in Laminar Flow Past Cavities", Journal of Heat Transfer, Vol.105, pp. 505-512.

Launder, B.E. and Spalding, D.B., 1974, "The Numerical Computation of Turbulent Flows", Computer Methods in Applied Mechanics and Engineering, Vol.3, pp. 269-289.

Launder, B.E. and Spalding, D.B., 1974, "The Numerical Computation of Turbulent Flows", Computer Methods in Applied Mechanics and Engineering, Vol.3, pp. 269-289.

Patankar, S.V., 1980, "Numerical Heat Transfer and Fluid Flow", Ed. Hemisphere Pub. Co., New York, EUA, 197 p.

Pereira, J.C.F. and Souza, J.M.M., 1995, "Experimental and Numerical Investigation of the Flow Oscillations in a Rectangular Cavity", Journal of Fluids Engineering, Vol.117, pp. 68-74.

Silveira Neto, A., Mattos, A. and Pinho, F.A.A., 1999, "Large-Eddy Simulation of Turbulent Flow Over a Two-Dimensional Cavity With Temperature Fluctuations", International Journal of Heat and Mass Transfer, Vol.42, pp. 49-59.

Sinha, S.N., Gupta, A.K. and Oberai, M.M., 1982, "Laminar Separating Flow Over Backsteps and Cavities. Part II: Cavities", AAIA Journal, Vol.20, pp. 370-375.

Wilcox, D.C., 1998, "Turbulence Modeling for CFD", DCW Industries, La Canadã, EUA, 460 p.

Zdanski, P.S.B., 2001, "Análise Numérica do Escoamento Incompressível Sobre Cavidades Rasas", MSc dissertation, Instituto Tecnológico de Aeronáutica, Brasil, 62 p.

Zdanski, P.S.B., Ortega, M.A. and Fico, N.G.C.R.Jr.,2000, "Numerical Simulation of Laminar Flow Over Shallow Cavities", Encit 2000, Porto Alegre, Brasil.